Fission Studies of Thorium, Uranium, and Plutonium Isotopes with (t, pf) Reactions*

J. D. Cramer and H. C. Britt
Los Alamos Scientific Laboratory, University of California, Los Alamos, New Mexico 87544
(Received 22 July 1970)

Experimental results are reported on fission probabilities and fragment angular correlations for (t,pf) reactions on ^{230}Th, ^{232}Th, ^{234}U, ^{236}U, ^{238}U, ^{238}Pu, ^{240}Pu, and ^{242}Pu targets. Systematic variations in the experimental results are used to qualitatively discuss properties of the fission barrier and low-lying transition-state spectra for these even-even nuclei.

I. INTRODUCTION

Direct reactions were first used by Northrop, Stokes, and Boyer[1] to determine the excitation energy of the fission barrier for the ^{236}U, ^{234}U, and ^{240}Pu compound nuclei. These even-even nuclei fission readily after their formation by the capture of a thermal neutron, indicating that the fission barrier lies below their neutron binding energies. The (d,pf) reaction on ^{235}U, ^{233}U, and ^{239}Pu target nuclei provides a mechanism for the excess energy of formation to be carried away from the nucleus in the kinetic energy of the outgoing proton. Fission cross sections can be measured by this technique from energies below the fission barrier to energies well above the neutron binding energy. Since this early work by Northrop, Stokes, and Boyer, several experiments utilizing arrays of semiconductor detectors have provided data from (d,pf) (t,pf), and (t,df) reactions.[2-7] Interpretation of the fragment angular distributions obtained from direct-reaction experiments is more complex than the interpretation of similar fission data obtained by neutron bombardment. In the neutron case the angular momentum transfer to the residual nucleus is distributed uniformly in a plane perpendicular to the incident neutron beam. In the direct-reaction process, the distribution of directions for the final angular momenta can be very complex and is sensitive to the detailed characteristics of the direct reaction. However, for incident bombarding energies near the Coulomb barrier when the outgoing direct particle is detected at far backward angles, it has been shown[2,3,8] that the angular momentum transfers are distributed approximately uniformly in a plane perpendicular to the kinematic recoil direction for the residual fissioning nuclei. The present experiments have been performed under conditions where this "plane-wave" approximation should be valid.

A survey of the properties of some even-even fissioning nuclei has been carried out previously using (d,pf) and (t,pf) reactions to induce fission in ^{234}U, ^{236}U, and ^{240}Pu nuclei. The work reported here is an extension of previous experiments,[2] providing an experimental survey of the fission barrier properties for all presently attainable even-even nuclei using the (t,pf) reaction. The (t,pf) reaction has several advantages over other direct reactions with significant cross sections. First, it is possible to reach a more neutron-rich part of the Periodic Table than for single-neutron transfer reactions. Second, in the study of even-even systems, the (t,p) reaction predominantly involves the transfer of two neutrons coupled to zero spin to a target with zero spin and, thus, the sensitivity of the angular correlations to the characteristics of the transition states contributing to fission is maximized. At energies above the neutron binding energy fission probabilities from the (t,pf) experiment are not significantly affected by projectile breakup reactions which cause difficulties in the interpretation of (d,pf) results.[7] Finally, (t,p) reactions on even-even nuclei excite only natural-parity states (positive-parity states of even angular momenta and negative-parity states of odd angular momenta) and this restricted class of excited states leads to simplification in the interpretation of the experimental results.

This paper presents experimental results on fission probabilities and fragment angular correlations for (t,pf) reactions on targets of ^{230}Th, ^{232}Th, ^{234}U, ^{236}U, ^{238}U, ^{240}Pu, and ^{242}Pu. The ^{234}U data have been previously published[2] but are included here for completeness. Some of these results have been described in more detail in a previous report,[9] and equivalent neutron cross sections deduced from the measured (t,pf) fission probabilities are reported in a separate publication.[10]

II. EXPERIMENTAL METHOD

The Van de Graaff facility at the Los Alamos Scientific Laboratory was used to provide the tri-

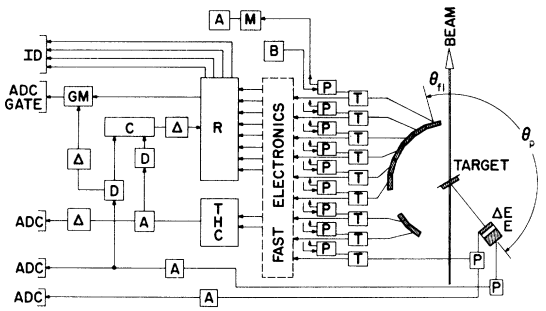

FIG. 1. Block diagram of "slow" electronics used in data acquisition system. Key to symbols: T – time-pick-off transformer, P – preamplifier, M – mixer for pre-amplifier signals, A – amplifier, R-ID – router and interface for identifying detector involved in a particular event, THC – overlap type time-to-amplitude converter, D – integral discriminator, Δ – variable delay unit, GM – gate monitor which generates gate signals for every coincidence event and for 1/100 of the single E events, ADC – analog-to-digital converter.

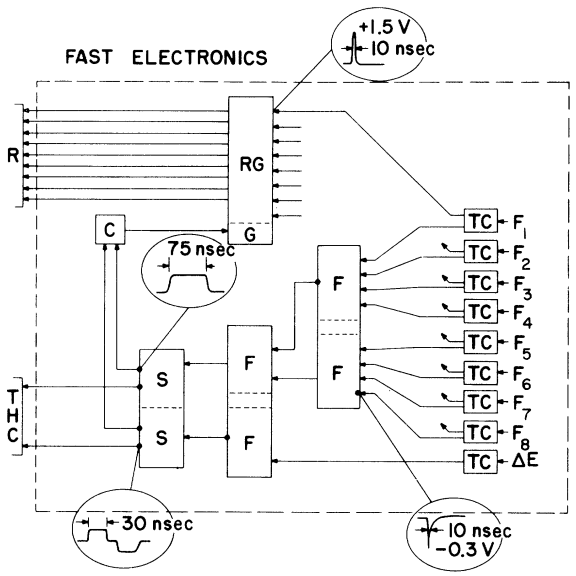

FIG. 2. Block diagram of "fast" electronics. Key to symbols: TC – time-pickoff control units, F – pulse fan-in, S – pulse shaper, C – fast coincidence, G – gate, RG – router gate.

ton beams used in these experiments. A beam energy of 18 MeV was used for all cases except ^{238}Pu, where the beam energy was 15 MeV. Targets were placed at the center of an array of eight fission-fragment detectors in a multipurpose scattering chamber as shown in Fig. 1. An E-ΔE charged-particle telescope was used to detect outgoing particles from the direct reaction at $\theta_p = 140°$ relative to the beam direction except for the ^{238}Pu(t, pf) results, where an angle $\theta_p = 115°$ was used. This angle is believed to be well within the angular region for the plane-wave approximation to be valid. The telescope consisted of a 200-μ surface-barrier transmission detector mounted in front of a 3-mm lithium-drifted detector. Fission fragments were detected in diffused-junction silicon detectors.

Targets were fabricated by evaporating a nominal 150–400-μg/cm^2 deposit of oxide material on thin (60 μg/cm^2) carbon backings. Table I lists the material composition of the targets.

The electronics and data reduction systems used in these experiments are modifications of the system described in more detail in a previous report.[9] The logic circuits used in the experiment are shown schematically in Figs. 1 and 2. Fast fission signals and ΔE signals from the time-pick-off transformers T were relayed to a mixer in the fast electronics circuits. At this point both fission and ΔE signals were split with one pair feeding a pulse overlap unit (THC) and the second pair triggering a coincidence gate trigger. If a coincidence was recorded the gate trigger allowed the fission event to be identified with a particular detector and this information was passed on to the interface of a SDS-930 computer. Coincident analog signals from the pulse overlap unit and the E detector provided a gate for the analog-to-digital converters (ADC). Analog signals from the pulse overlap unit, and the E and ΔE amplifiers

TABLE I. Target materials. All backing material 60–70-μg/cm^2 carbon.

Target isotope	Weight fraction	Contaminants – weight fraction	Areal density of oxide (μg/cm^2)
^{230}Th	0.8982	^{232}Th-0.1018	260
^{232}Th	1.000	None	200
^{234}U	0.997	^{235}U-0.003	200
^{236}U	0.9988	^{235}U-0.0012	200
^{238}U	0.9997	^{235}U-0.0003	~200
^{238}Pu	0.9948	^{239}Pu-0.0046, ^{240}Pu-0.0004	40
^{240}Pu	0.9800	^{239}Pu-0.0119; ^{242}Pu-0.0016; ^{241}Pu-0.0065	240
^{242}Pu	0.9988	^{239}Pu-0.0002; ^{240}Pu-0.0004; ^{241}Pu-0.0006	330

were read into the computer through the ADC. In addition to the coincidence data, a simultaneous record of the direct-reaction cross section was made using a separate gate signal from the E detector to record 1% of the singles (noncoincident) events.

A preliminary data reduction was performed in the on-line SDS computer to provide a continuous observation of the data as they were recorded. All of the gated events were also recorded on magnetic tape and the final data reduction was performed on a CDC-6600 computer at a later time. All direct-reaction fission events which are possible using the incident 18-MeV triton beam were recorded. The reactions observed in this experiment were (t, pf), (t, df), and $(t, t'f)$. The (t, df) results are reported in a report in systematics of fission of odd-A nuclei[7] and the cross sections for $(t, t'f)$ reactions were so low that significant data were not obtained. The analog signals from the E-ΔE detectors were used to identify the reaction by determining the mass of the detected particle. A standard mass identification scheme[11] based on the range-energy relationship in silicon was used to generate a mass spectrum and each reaction can be analyzed separately from this point. Pulse amplitudes from the THC can be used to distinguish real and accidental coincidence events and for each detector coincidence spectra are corrected for accidental contributions. A series of three coincidence runs providing fragment angular-distribution data for a total of 24 fission detector positions were acquired for each target with the exception of ^{232}Th and ^{238}Pu. Only 16 detector positions were used in these cases.

In addition to the normal coincidence mode of operation described above, a short series of energy calibration runs was interspersed where the E-ΔE detectors were moved as far away from the target as possible to reduce kinematic broadening of the known energy peaks from the reactions on ^{12}C and ^{16}O nuclei in the target. Several angles θ_p were used to kinematically change the position of each peak. From the known excitation energy of these peaks and the computed kinematic shifts, the kinetic energy of the outgoing particle can be calculated and provides several energy calibration points for the coincidence data.

The over-all energy resolution of the experiments as measured from the full width at half maximum on the triton-elastic peak is 110–120 keV.

The relative efficiencies of the fission detectors were determined for each array geometry by recording the relative numbers of triton-induced fission events in each detector. These data were obtained in separate short runs with low-beam current in identical fission detector geometries to the coincidence runs. When these data were corrected for the measured laboratory angular distribution for the (t, f) reactions on the specific target, the relative efficiency of each detector could be determined.

The coincidence spectra, which have been corrected for accidental background, are converted to 50-keV intervals of nuclear excitation energy from the measured energy of the outgoing direct-reaction product and the reaction Q value. The Q values were measured for the (t, p) reactions on all of the targets[12] except ^{230}Th and ^{238}Pu. All of the experimental data for each nucleus is then represented by a normalized three-dimensional array of corrected coincidence counts, nuclear excitation energy, and detector position in center-of-mass angles relative to the recoil direction.

Qualitative interpretation of this information requires a more compact form of representation than exists in the three-dimensional data arrays. One very useful method of representing these experimental data is to fit the arrays $W(\theta, E)$ to a series of even Legendre polynomials $P_L(\cos\theta)$,

$$W(\theta, E) = A_0(E)\left[1 + \sum_{L=2,4,6\ldots}^{12} g_L(E) P_L(\cos\theta)\right], \quad (1)$$

allowing the variation of the parameters A_0 and

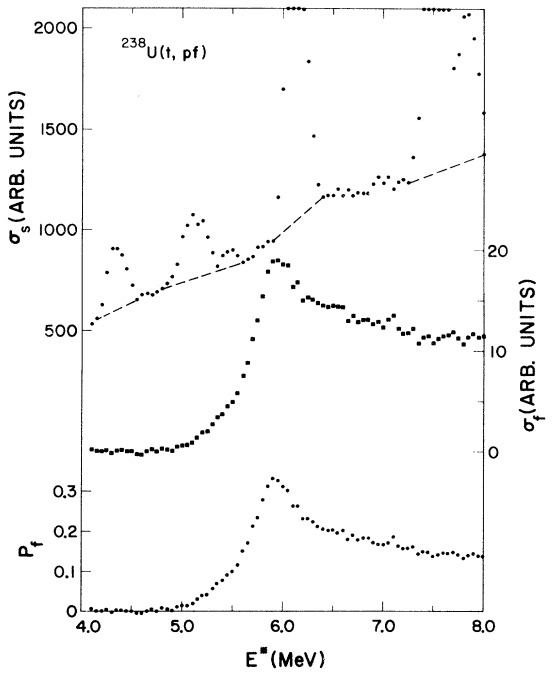

FIG. 3. Singles proton spectra σ_s and coincidence proton spectra σ_f with resultant fission probability $P_f = \sigma_f / \sigma_s$. Dashed lines in the singles spectra represent extrapolations of the (t, p) cross sections underneath peaks created by (t, p) reactions on ^{12}C and ^{16}O.

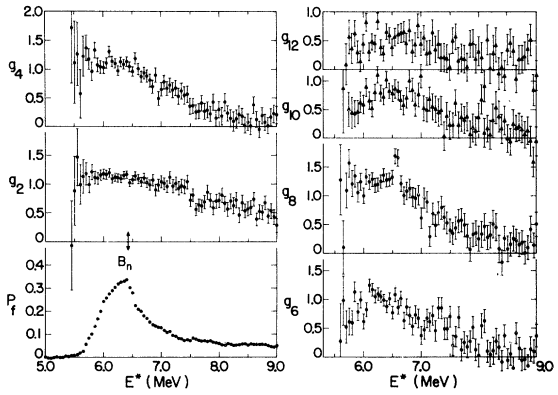

FIG. 4. Fission probability and angular-correlation coefficients for the ^{230}Th(t,pf) reaction.

the g_L's to fit the angular data at 50-keV intervals. The fitting procedure accounts for the finite solid angle of the detectors by integrating the Legendre polynomials in the series over the detector solid angle to obtain the computed function. Even L values up to 12 are necessary in the series to achieve an optimum fit.

Experimentally, A_0 represents a fission cross section σ_f in arbitrary units – the fraction of the total fission events which were observed in the fraction of solid angle $\Delta\Omega/4\pi$ subtended by the standard fission detector for the duration of the experiment. The probability P_f that a fission will occur if the nucleus is excited to energy E by a (t,p) reaction can be ascertained from the ratio of A_0 to the number of (t,p) reactions N_s observed in the singles spectrum. Specifically for this experiment,

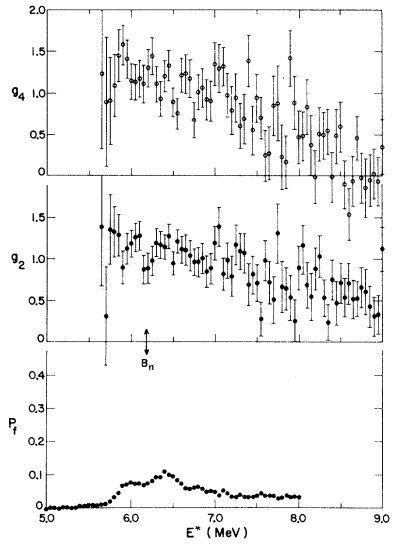

FIG. 5. Fission probability and angular-correlation coefficients for the ^{232}Th(t,pf) reaction.

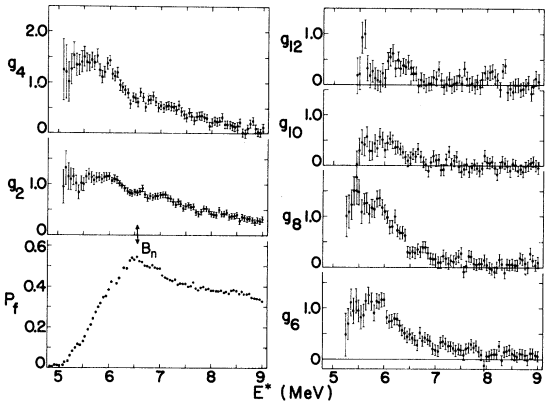

FIG. 6. Fission probability and angular-correlation coefficients for the ^{234}U(t,pf) reaction.

$$P_f(E)=\frac{1}{2}\left(\frac{4\pi}{\Delta\Omega}\right)\frac{A_0(E)}{100N_s(E)}. \quad (2)$$

The factor $\frac{1}{2}$ reflects the fact that there are two fragments emitted per fission event, and the factor of 100 before N_s is a prescaling factor set on the ADC gate trigger to limit the number of recorded singles events.

The various quantities used in this analysis are shown in Fig. 3. The fission cross section σ_f is just A_0 and the (t,p) cross section σ_s is just the singles spectrum N_s. The dashed lines in σ_s indicate the interpolated value of the (t,p) cross section on ^{238}U used to calculate P_f. The sharp peaks in the spectrum are the carbon and oxygen peaks which must be eliminated for this analysis. The value of A_0 versus excitation energy is shown in the central plot (indicated by square plotting characters) and P_f, the result of Eq. (2), is shown at the bottom of this figure.

All of the experimental fragment angular-distribution data are contained in the six energy dependent angular-correlation coefficients of Eq. (1).

III. EXPERIMENTAL RESULTS

The fragment angular-correlation coefficients and the fission probabilities for all nuclei studied are shown in Figs. 4 through 11. Error bars in these plots represent statistical errors reflecting the number of counts observed at each detector position and serve only to indicate the expected point-to-point fluctuation of the data. Uncertainties of ±10% are assigned to the absolute value of the fission probabilities reflecting the uncertainty in the measured solid angle of the fission detector, dead time in electronic apparatus, and relative normalizations of combined runs in addition to the statistical fluctuations indicated in the figures. Additional uncertainties in the angular-distribution

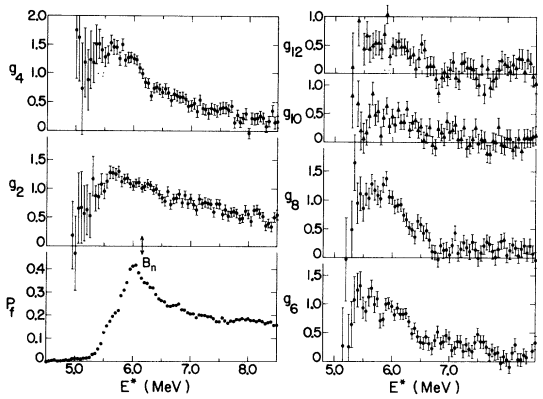

FIG. 7. Fission probability and angular-correlation coefficients for the ^{236}U(t,pf) reaction.

data are small compared with the indicated statistical errors and include uncertainties in relative detector efficiency and relative normalizations of combined data. The neutron binding energies for all eight nuclei are indicated by the arrow labeled B_n on each plot.

A typical characteristic of these data is a rise in the fission probability as more excitation energy is supplied to the nucleus, until the neutron binding energy is reached. The indication of the opening of new transition states is suggested by correlated structure observed in both the fission probability and the angular-correlation coefficients as the barrier is surmounted.

At the neutron binding energy, neutron emission becomes energetically possible and strongly competes with the fission and γ-decay processes, resulting in a sharp drop and continued decrease in the fission probability at that point. Below the nucleon pairing energy (~2 MeV), only collective transition states are present in the vicinity of the fission barrier and the fission fragment anisotropies are sensitive indicators of the appearance of each new state and its respective K value. Members of the $K^\pi = 0^+$ rotational band are the lowest-lying barrier states for even-even nuclei. Fission through these levels is characterized by forward peaking of the fragments corresponding to the large values for the angular-correlation coefficients g_L observed in all of the data as fission first becomes probable. Similarly the $K^\pi = 0^-$ band – the mass-asymmetry vibrational mode – is characterized by large g_L values. In principle, $K = 0^+$ and 0^- can be distinguished because for a $K = 0^+$ band values of g_4, g_8, and g_{12} should be larger than values of g_2, g_6, and g_{10} and the reverse is true for a $K = 0^-$ band. This characteristic is a direct result of the selection of natural-parity states by the (t,p) reaction. As the higher K bands enter, successive decreases in the fragment anisotropies are observed.

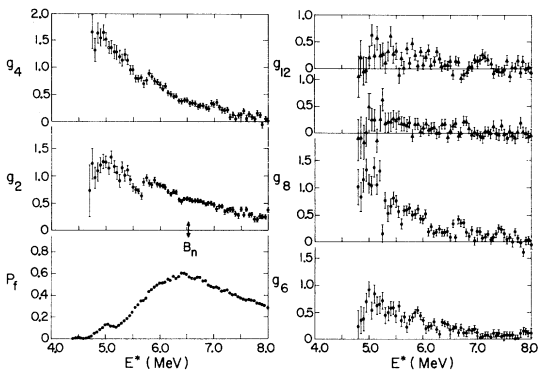

FIG. 9. Fission probability and angular-correlation coefficients for the ^{238}Pu(t,pf) reaction.

The experimental fission probabilities for each nucleus studied are also shown in the semilog plots of Figs. 12–14. Of particular interest in these plots are the similarities in sub-barrier structure which occur in these data and the (d,pf) data.[2,3,13] The ^{240}Pu sub-barrier resonance at 5.0 MeV in Fig. 5 has been previously reported from both (d,pf)[2,3,13] and $(p,p'f)$[14] experimental work.

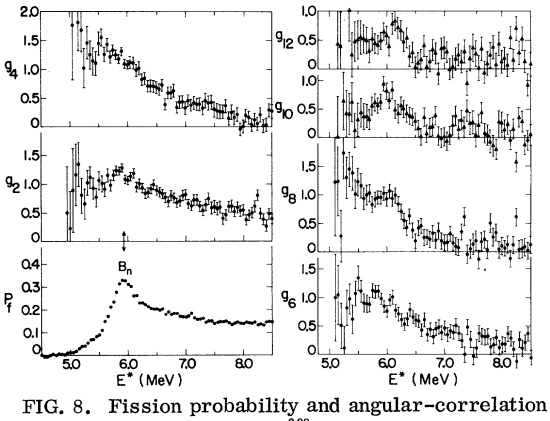

FIG. 8. Fission probability and angular-correlation coefficients for the ^{238}U(t,pf) reaction.

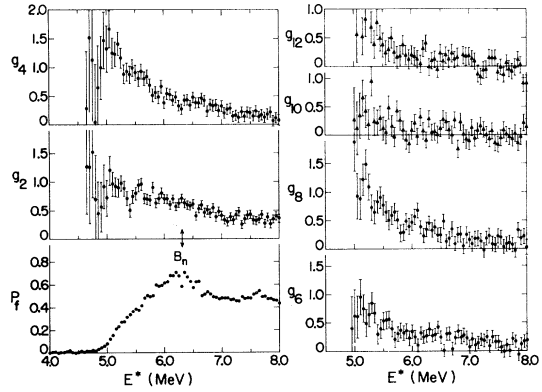

FIG. 10. Fission probability and angular-correlation coefficients for the ^{240}Pu(t,pf) reaction.

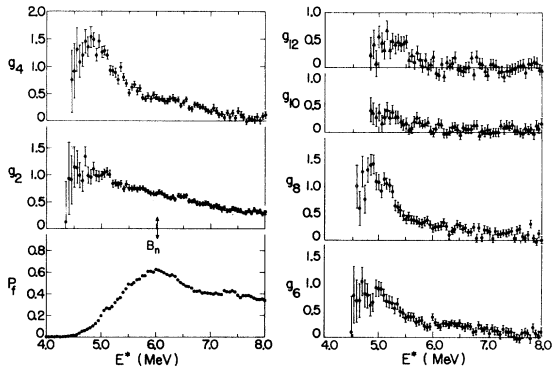

FIG. 11. Fission probability and angular-correlation coefficients for the ^{242}Pu(t,pf) reaction.

^{239}Pu(d,pf) results reported by Pedersen *et al.*[13] indicate an additional sub-barrier peak at 4.5 MeV which is also apparent in the ^{238}Pu(t,pf) results of Fig. 14.

Although statistical errors are large, there appears to be evidence of two subthreshold peaks in the ^{240}Pu(t,pf) results confirming the ^{241}Pu(d,pf) results[13] which also indicate double subthreshold resonances. Futhermore, it is seen in the ^{234}U(t,pf) data in Fig. 4 that a plateau exists at 5.05 MeV. This feature is also evident in the (d,pf) data.[13] These sub-barrier structures are currently believed to represent the enhanced transmission due to the influence of quasibound levels in an intermediate well in the fission barrier.

The significant general features of the data for each nucleus including important differences between nuclei are discussed in the remainder of this section.

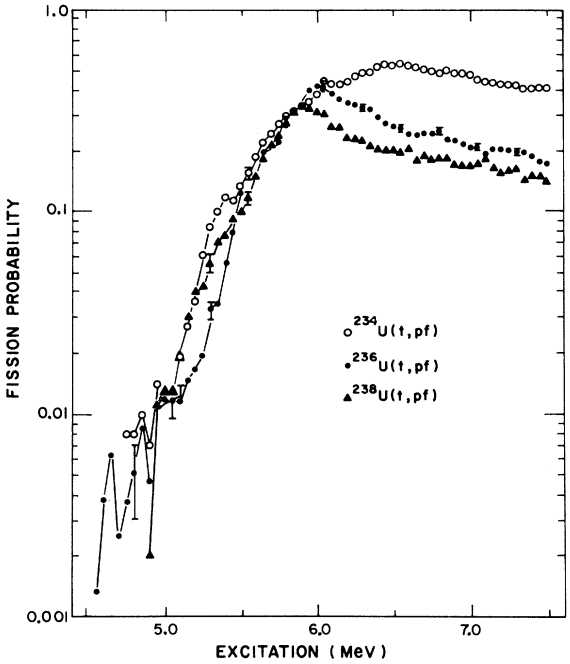

FIG. 13. Fission probabilities from (t,pf) reactions on ^{234}U, ^{236}U, and ^{238}U targets.

1. Thorium Nuclei

Two facts are immediately apparent upon inves-

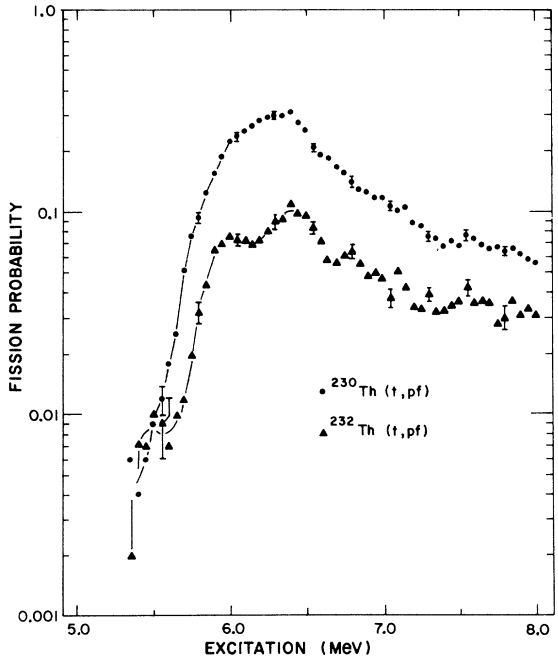

FIG. 12. Fission probabilities from (t,pf) reactions on ^{230}Th and ^{232}Th targets.

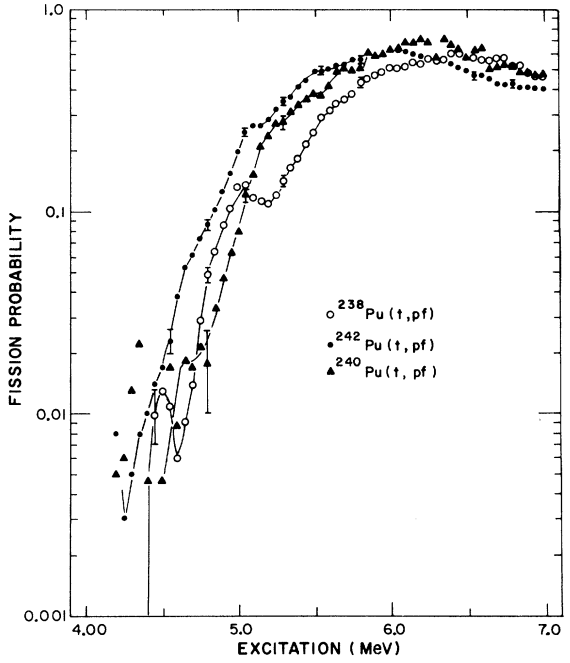

FIG. 14. Fission probabilities from (t,pf) reactions on ^{238}Pu, ^{240}Pu, and ^{242}Pu targets.

tigation of the thorium data in Figs. 4, 5, and 12. The ^{234}Th nucleus is not readily fissionable as indicated by the very small fission probability for ^{232}Th(t,pf), and as a direct result of this fact, the statistical errors in the angular-distribution data are very large. An interesting anomaly is displayed in the ^{234}Th fission probability; after rising to a slight peak below the neutron binding energy, the fission probability continues to increase above the neutron binding energy. Two explanations are possible. The first peak could result from a sub-barrier resonance in the penetrability or, alternatively, the neutron binding energy lies between the $K=0^+$ and $K=0^-$ bands. Both situations could produce the observed effect. Both ^{232}Th and ^{234}Th are distinguished by the persistence of the large angular-correlation coefficients above the fission barrier.

2. Uranium Nuclei

The fission probabilities of all of the uranium nuclei shown in Figs. 6–8 and 13 are similar with the only major difference produced by the variation of the neutron binding energy from ^{236}U to ^{240}U. The fission barrier for these three nuclei must be very similar. Angular-correlation coefficients display the early rise due to the $K=0^{\pm}$ states; however, in contrast to the thorium data, at $E^*\sim 6.0$–6.5 MeV, a sharp decrease is apparent especially in g_4 and g_8, indicating the opening of bands with $K\geq 2$ at an energy of ~0.5 MeV above the fission barrier.

3. Plutonium Nuclei

The plutonium nuclei are the most fissionable of all of the nuclei studied here as seen by the large fission probabilities in Figs. 9–11 and 14. The neutron binding energy in these plutonium isotopes is well above the fission barrier allowing the fission probability to rise higher than the others before neutron emission occurs. For the plutonium isotopes the angular-correlation coefficients also show a sharp decrease indicating the opening of $K\geq 2$ states and in this case these states become important to energies of ~0.2–0.3 MeV above the fission threshold. The results from ^{238}Pu(t,pf) are compared with ^{239}Pu(d,pf) and ^{240}Pu$(p,p'f)$ results,[2,14] in Fig. 15. The correspondence of a strong dip in g_2 at ~5.5 MeV in both the (t,pf) and (d,pf) results supports the previous hypothesis[2,14] that this structure is caused by the opening of a $K=2^+$ band followed by the $K=0^-$ band. This conclusion is strengthened by the (t,pf) results which show the peak at ~5.8 MeV is more prominent in g_2 than in g_4.

IV. DISCUSSION

In order to obtain detailed information on the properties of the fission barrier and the transition-state spectra from the (t,pf) data, the results must be compared with a detailed model of the direct-reaction fission process. Preliminary attempts at such a comparison[9] have indicated qualitative agreement between calculation and experiment but the uniqueness of the shapes of the double-peaked barrier determined was in doubt because of the large number of parameters necessary to describe such a barrier. In addition, comparisons of model calculations and experimental results for the ^{239}Pu(d,pf) reaction[13,14] have indicated the necessity of including damping in the secondary minimum of the fission barrier and the possibility that the K quantum number may not always be conserved over the entire region of penetration of the fission barrier. Also it has been demonstrated[13,14] that the detailed interpretation of the direct-reaction fission results is very sensitive to the assumptions made concerning the characteristics of the direct-reaction process. It is hoped that in the future realistic theoretical barrier shapes[15] can be coupled with a better understanding of the direct-reaction process and data from fission isomer studies[16] to give a qualitative interpretation of the experimental results.

Even though detailed analyses have not yet been

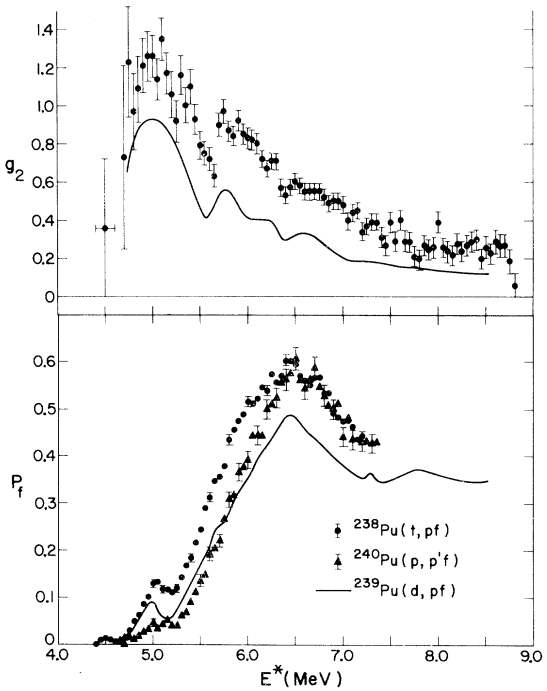

FIG. 15. Fission probabilities and angular-correlation coefficients g_2 for (t,pf), (d,pf), and $(p,p'f)$ reactions leading to the fissioning system ^{240}Pu.

obtained, this experimental survey illustrates several general trends in the fission process as one scans from thorium to plutonium in the actinide region. First, sub-barrier structure in P_f provide evidence of a resonance in the intermediate well in the fission barrier in virtually all of the nuclei studied. Even where resonant structure is not apparent near the barrier peaks, knees or changes in slope appear in the fission probabilities for some of the nuclei studied.

Some conclusions about general trends in the transition-state spectra for these nuclei can also be made from a qualitative examination of the angular-correlation coefficients. The sharp decrease which is most evident in the g_4 and g_8 coefficients is characteristic of the onset of fission through $K=2^+$ transition states. The results indicate that the $K=2^+$ vibration increases in energy as Z^2/A decreases from plutonium to uranium. In the thorium nuclei the $K=2^+$ vibration has either further increased in energy or the shape of the fission barrier has changed to give a second peak which is higher than the first peak and tends to favor $K=0$ states for a considerable energy region above the apparent threshold. This systematic variation of the $K=2^+$ vibrational energy is consistent with previous analysis of (d,pf) results[2] and with recent theoretical calculations.[17]

Limited information on the $K=0^-$ band can be obtained using the fact that the (t,pf) reaction fission through a $K=0^+$ band should give $g_2 \sim 1.0$ and $g_4 \sim 1.5$, while equal contributions from $K=0^+$ and $K=0^-$ bands give $g_2 = g_4 \sim 1.2$. In the plutonium nuclei the peak in g_2 and g_4 in the region $E^* \sim 5.5$–6.0 MeV indicates that the $K=0^-$ vibrational energy is slightly greater than the $K=2^+$ energy, while for thorium nuclei the g_2 and g_4 coefficients indicate that the $K=0^+$ and $K=0^-$ bands are almost degenerate in energy. These results indicate that the $K=0^-$ vibrational energy decreases as Z^2/A is decreased from plutonium to thorium. This trend is consistent with the analysis of previous results,[2] with the interpretation of photofission data[18] and with theoretical liquid-drop calculations.[19]

These trends in the $K=2^+$ and $K=0^-$ vibrational energies are illustrated more quantitatively in attempts[9] to fit the experimental results with a semiquantitative model of the direct-reaction process employing fission through a double-peaked barrier. This model and fits to a variety of experimental data are presently being refined and will be reported in detail in the future.

ACKNOWLEDGMENTS

We gratefully acknowledge helpful discussions with J. R. Nix and S. Bjørnholm. We would like to thank F. A. Rickey, Jr., and S. C. Burnett for assistance in the data collection and W. S. Hall for help in preparing some of the computer programs used in the data analysis. We are grateful to J. S. Levin and M. P. Kellogg for writing the on-line data acquisition programs. We would like to thank G. Sletten and S. Bjørnholm for loaning us the ^{238}Pu target and Judith C. Gursky and J. G. Povelites for preparing the other targets.

---

*Work performed under the auspices of the U. S. Atomic Energy Commission.

[1]J. A. Northrop, R. H. Stokes, and K. Boyer, Phys. Rev. 115, 1277 (1959).

[2]H. C. Britt, F. A. Rickey, Jr., and W. S. Hall, Phys. Rev. 175, 1525 (1968).

[3]H. C. Britt, W. R. Gibbs, J. J. Griffin, and R. H. Stokes, Phys. Rev. 139, B354 (1965).

[4]R. Vanderbosch, J. P. Unik, and J. R. Huizenga, in *Proceedings of the Symposium on the Physics and Chemistry of Fission, Salzburg, 1965* (International Atomic Energy Agency, Vienna, Austria, 1965), Vol. I, p. 547.

[5]H. J. Specht, J. S. Fraser, and J. C. D. Milton, Phys. Rev. Letters 17, 1187 (1966).

[6]D. Eccleshall and M. H. C. Yates, in *Proceedings of the Symposium on the Physics and Chemistry of Fission, Salzburg, 1965* (International Atomic Energy Agency, Vienna, Austria, 1965), Vol. I, p. 77.

[7]H. C. Britt and J. D. Cramer, Phys. Rev. (to be published).

[8]K. L. Wolf, R. Vanderbosch, and W. D. Loveland, Phys. Rev. 170, 1059 (1968).

[9]J. D. Cramer, Los Alamos Scientific Laboratory Report No. LA-4198, 1969 (unpublished).

[10]J. D. Cramer and H. C. Britt, Nucl. Sci. Eng. 41, 177 (1970).

[11]D. D. Armstrong, J. G. Beery, E. R. Flynn, W. S. Hall, P. W. Keaton, Jr., and M. P. Kellogg, Nucl. Instr. Methods 70, 69 (1969).

[12]H. C. Britt and J. D. Cramer, Phys. Rev. 185, 1553 (1969).

[13]J. Pedersen and B. D. Kuzminov, Phys. Letters 29B, 176 (1969); B. B. Back, J. P. Bondorf, G. A. Otroschenko, J. Pedersen, and B. Rasmussen, in *Proceedings of the Second International Atomic Energy Symposium on Physics and Chemistry of Fission, Vienna, Austria, 1969* (International Atomic Energy Agency, Vienna, Austria, 1969), p. 351.

[14]H. C. Britt, S. C. Burnett, and J. D. Cramer, in *Proceedings of the Second International Atomic Energy Symposium on Physics and Chemistry of Fission, Vienna, Austria, 1969* (International Atomic Energy Agency, Vienna, Austria, 1969), p. 375.

[15]J. R. Nix, A. M. Bolsterli, and E. O. Fiset, private

communication.
[16]S. C. Burnett, H. C. Britt, B. H. Erkkila, and W. E. Stein, Phys. Letters 31B, 523 (1970).
[17]M. Zielinska-Pfabe, Phys. Letters 29B, 280 (1969).
[18]S. P. Kapitza, N. S. Rabotnov, G. N. Smirenkin, A. S. Soldatov, L. N. Usachev, and Yu. M. Tsipenyuk, Zh. Eksperim. i Teor. Fiz. – Pis'ma Redakt 9, 128 (1969). [transl.: JETP Letters 9, 73 (1969)].
[19]J. R. Nix, Ann. Phys. (N.Y.) 41, 52 (1967).

PHYSICAL REVIEW C VOLUME 2, NUMBER 6 DECEMBER 1970

Studies of the Radioactive Decays of ^{152}Eu and ^{154}Eu

L. L. Riedinger* and Noah R. Johnson
Oak Ridge National Laboratory,† Oak Ridge, Tennessee 37830
and
J. H. Hamilton
Physics Department, Vanderbilt University,‡ Nashville, Tennessee 37203
(Received 6 April 1970; revised manuscript received 3 August 1970)

γ rays emitted in the radioactive decays of ^{152}Eu and ^{154}Eu have been studied with Ge(Li) and NaI detectors. Energies and relative intensities were derived from singles experiments with large volume Ge(Li) detectors and assignments of γ rays to transitions in the level schemes were made with the help of Ge(Li)-NaI coincidence measurements. In all, 71 γ rays were observed in the ^{152}Eu decay and 51 in the ^{154}Eu case. Three members of each of the β- and γ-vibrational bands were observed. In addition the results of the coincidence experiments are used to assign a level at 1649.8 keV as the probable 2^- member of the $K=2$ band in ^{152}Sm. The properties of this state and of the $K^\pi=0^-$ and 1^- bands are compared with the properties of the corresponding states in ^{154}Gd. It is found that there is evidently less Coriolis coupling between the negative-parity states in ^{152}Sm than in ^{154}Gd. The members of the $K^\pi=1^-$ band in the former are not inverted as in the latter, and the $B(E1)$ ratios from the $K^\pi=0^-$ states in the former are in better agreement with the predictions of the rotational model. The low-energy levels in ^{152}Gd are considered in light of two possible interpretations. We find that it is preferable to consider these states as resulting from quasirotations and quasivibrations than to treat them as members of one-, two-, and three-phonon vibrational excitations about spherical equilibrium shapes. Finally, a new 2^+ level at 1293 keV in ^{152}Sm is discussed in light of recent experiments involving two-neutron-transfer reactions to levels in this nucleus.

I. INTRODUCTION

The onset of nuclear deformation is rather abrupt at the beginning of the rare-earth region of deformed nuclei. The ^{152}Gd nucleus with 88 neutrons has been characterized as nearly spherical in shape, partially on the basis of a vibrational-like spectrum. The $N=90$ nuclei, for example ^{152}Sm and ^{154}Gd, display the low-lying excited states characteristic of rotational spectra and are considered to be deformed. However, these three nuclei are better referred to as transitional, since their properties preclude classification as well-formed spherical or deformed nuclei. For example, the first excited state of ^{152}Gd occurs at 344 keV, lower than expected for a quadrupole vibration about a spherical shape. The levels of the rotational spectra of ^{152}Sm and ^{154}Gd deviate more widely from the $I(I+1)$ energy spacings expected for rigid rotators than do the levels in heavier rare-earth nuclei. Also, the quadrupole-vibrational states of the two latter nuclei are found at lower energies than the corresponding levels in the heavier nuclei. Comparative studies of these three nuclei can lead to a wealth of information concerning collective effects in transitional nuclei, and thus several years ago we initiated experiments on the γ rays emitted in the radioactive decays of ^{152}Eu and ^{154}Eu.

Some preliminary results of this work have been published.[1] Many additional investigations of these level schemes have been performed, as reported earlier.[2] In recent years, particularly during the course of our work, other studies have been reported by Dzhelepov and his coworkers,[3-6] Liu *et al.*,[7] and Varnell, Bowman, and Trischuk (VBT),[8] who have investigated the ^{152}Sm, ^{152}Gd, and ^{154}Gd excitation spectra through radioactive decay techniques. Bisgaard, Nielsen, and Sodemann (BNS),[9] Katoh and Spejewski,[10] Malmsten, Nilsson, and